


Cite this: *RSC Adv.*, 2019, 9, 40176

## Nitric oxide diffusion through cystic fibrosis-relevant media and lung tissue†

Jackson R. Hall, Sara E. Maloney, Haibao Jin, James B. Taylor  
and Mark H. Schoenfisch \*

A simplified diffusion cell methodology was employed to measure the diffusion coefficient of nitric oxide (NO) through phosphate buffered saline (PBS) and artificial sputum medium (ASM)—an *in vitro* analog for airway mucus. Diffusion through the proteinaceous ASM yielded a significantly lower diffusion coefficient compared to PBS, which is attributed to both the physical obstruction by the mucin mesh and reactive nature of NO radicals towards the biological compounds in ASM. To further confirm that ASM was restricting NO from diffusing freely, a macromolecular propylamine-modified cyclodextrin donor (CD-PA) was employed to release the NO more slowly. The NO diffusion characteristics in ASM *via* the NO donor were also slower relative to PBS. As NO is likely to interact with lung cells after passing through the mucus barrier, the diffusion of both NO and the CD-PA macromolecular NO donor through differentiated lung tissue was investigated with and without an ASM layer. Comparison of NO diffusion through the three diffusion barriers indicated that the lung tissue significantly impeded NO penetration over the course of the experiment compared to PBS and ASM. In fact, the diffusion of CD-PA through the lung tissue was hindered until after the release of its NO payload, potentially due to the increased net charge of the NO donor structure. Of importance, the viability of the tissue was not influenced by the NO-releasing CD-PA at bactericidal concentrations.

Received 12th September 2019  
Accepted 24th November 2019

DOI: 10.1039/c9ra07367a

rsc.li/rsc-advances

Cystic fibrosis (CF) is an inherited disease caused by a defect in the CF transmembrane conductance regulator protein (CFTR).<sup>1–4</sup> As a result, chloride ion transport facilitated by the CFTR is impeded, reducing water transport and concentrating the mucus lining in the lungs.<sup>5</sup> Over time, mucins, the main protein component of mucus, and DNA, released from neutrophils during the inflammatory response, accumulate and obstruct mucociliary clearance.<sup>6,7</sup> Dense, stagnant mucus in the lungs of CF patients provides an optimal environment for bacterial colonization. Ample nutrients and the protection afforded by the mucus layer promote biofilm formation, which are complex communities of pathogenic bacteria encased in an exopolysaccharide matrix.<sup>1,3,5</sup> Biofilms hinder drug diffusion, alter bacterial metabolism, and increase tolerance towards traditional antibiotics.<sup>1,8,9</sup> As such, severe chronic infections persist in the lungs of CF patients, requiring the constant administration of antibiotics (*e.g.*, colistin and tobramycin) to mitigate infections and prolong the lives of those afflicted with CF.<sup>3,10,11</sup>

The continuous administration of antibiotics required to combat these chronic infections has led to the rapid rise of

multi-drug resistant (MDR) bacteria in the CF community, necessitating the development of novel therapeutics.<sup>12,13</sup> Nitric oxide (NO), an endogenously produced free radical, is capable of inducing both oxidative and nitrosative stress (*e.g.*, damaging membrane proteins and DNA, lipid peroxidation) to eradicate bacteria.<sup>14–16</sup> The multi-mechanistic antibacterial action significantly diminishes the risk of inducing bacterial resistance.<sup>14,17</sup> In addition to acting as a broad-spectrum antibiotic, NO has been shown to function as a mucolytic agent.<sup>18,19</sup> This dual activity makes NO an appealing potential therapeutic for addressing both chronic biofilm infections and the highly viscoelastic mucus that together contribute to the morbidity and mortality of CF patients.

While NO's therapeutic potential is immense, it naturally exists as a highly reactive radical in aqueous solutions. Metal ions, proteins with heme centers (*e.g.*, hemoglobin), and oxygen readily react with and consume free NO, reducing the concentrations available for therapeutic action.<sup>20–23</sup> As such, the lifetime of NO is approximated to be only a few seconds in proteinaceous media.<sup>24,25</sup> Although the literature has modeled and calculated diffusion coefficients for NO through water, saline solutions, various gas permeable polymers, and select biological components (*e.g.*, lipid membranes), reports often stop short of determining behavior in complex biological solutions.<sup>26–31</sup> With respect to CF, mucus is well-known to act as a barrier to traditional drug delivery *via* physical hinderance

Department of Chemistry, The University of North Carolina at Chapel Hill, Chapel Hill, North Carolina, 27599, USA. E-mail: schoenfisch@unc.edu

† Electronic supplementary information (ESI) available. See DOI: 10.1039/c9ra07367a



and hydrophobic interactions.<sup>32,33</sup> Nitric oxide's diffusion through complex, protein-rich solutions is especially susceptible to scavenging, severely impeding its penetration and antibacterial efficacy. Understanding the diffusive capabilities of NO through the mucus barrier is thus vital to CF therapeutic design and dosage. Herein, we utilized a custom side-by-side diffusion cell to compare the diffusion coefficients of NO through a simple solution (*e.g.*, phosphate buffered saline; PBS) with a CF-relevant, proteinaceous solution (*e.g.*, artificial sputum medium; ASM) in order to quantify how the increased complexity of mucus impacts the movement of free NO.

Delivery of NO in its gaseous form introduces multiple barriers (*e.g.*, toxicity, lack of extended release, systemic effects) for effective treatment, which has resulted in the development of NO donor-modified macromolecular scaffolds.<sup>34–36</sup> We have previously described NO-releasing biopolymers to reduce cytotoxicity and potentially enable natural biodegradation pathways to clear the drug, while also providing large NO payloads, extended release, and targeted therapy.<sup>37–39</sup> The diffusion of NO released from a biopolymeric scaffold through simple and complex media (PBS and ASM, respectively) was examined using a diffusion cell methodology. Differences in the rate of NO diffusion through PBS and ASM provided insight into NO's potential interactions with these fluids. In the CF airway, NO that diffuses across the mucus barrier is expected to interact with the epithelial lung tissue. To further explore NO's diffusion and cytocompatibility, a bactericidal dose of a macromolecular NO donor (*i.e.*, NO-releasing cyclodextrin) was exposed to *in vitro* lung tissue with monitoring of both NO and the biopolymer through this complex barrier. Toxicity to the lung tissue was also evaluated to determine any impact of bactericidal concentrations of the NO donor.

## Experimental

### Materials

Sulfanilamide, hydrochloric acid (HCl), sodium nitrite standard, *N*-(1-naphthyl)ethylenediamine dihydrochloride (NED), casamino acids, gastric pig mucin type II (GPM), and Tris base were purchased from Millipore Sigma (St. Louis, MO). Phosphoric acid, phenazine methosulfate (PMS), dialysis tubing, deoxyribonucleic acid sodium salt (DNA; fish sperm), egg yolk emulsion, sodium chloride, potassium chloride, and diethylenetriaminepentaacetic acid (DTPA) were acquired from Fisher Scientific (Fair Lawn, NJ). The 3-(4,5-dimethylthiazol-2-yl)-5-(3-carboxymethoxyphenyl)-2-(4-sulfo-phen-yl)-2H-tetrazolium inner salt (MTS) was purchased from Promega (Madison, WI). Nitric oxide (99.5%) and argon (Ar; 99.995%) gas cylinders were purchased from Airgas National Welders (Durham, NC). Distilled water was purified (18.2 MΩ cm and ≤6 ppb total organic content) with a Millipore Milli-Q UV gradient A10 system (Bedford, MA). All absorbance values were measured using a SpectraMax M2e microplate spectrophotometer (Molecular Devices; Sunnyvale, CA).

Saturated NO solutions were prepared by deoxygenating 25 mL of phosphate buffered saline (PBS; 10 mM, pH 7.4) with Ar gas for 25 min over ice. Then, NO gas was bubbled through

for 25 min at 0 °C to generate ~2.0 mM NO solution. The saturated NO solution was used the same day as prepared. Artificial sputum medium (ASM) was prepared according to established protocols.<sup>40,41</sup> For 1 L of ASM, DNA (4 g), GPM (5 g), DTPA (5.9 mg), NaCl (5 g), KCl (2.2 g), Tris base (1.81 g), and casamino acids (5 g) were dissolved in 800 mL of water. Tris base (1.0 M) was used to adjust the pH of the solution to pH 6.5, and the solution was further diluted to 1 L. An autoclave was used to sterilize the ASM and allowed to cool, after which, 5 mL of egg yolk emulsion was added under sterile conditions. The ASM was stored at 4 °C until use.

### Synthesis of NO-releasing cyclodextrin (CD-PA/NO)

Propylamine-modified β-cyclodextrin (CD-PA) was synthesized as previously reported.<sup>38</sup> Briefly, β-cyclodextrin (CD) was dissolved in a basic solution and reacted with *p*-toluenesulfonyl chloride (added dropwise) for 3 h at room temperature. The resulting mono-substituted CD was precipitated by lowering the pH to 9.0 and filtered. The recovered solid was redissolved in water and stirred with propylamine for 3 d at 75 °C. The product was precipitated in acetone, washed, and dried for 3 d. *N*-diazoniumdiolates were appended onto the CD-PA by dissolving the solid in 1 : 1 H<sub>2</sub>O : MeOH with 5 equivalents of sodium methoxide per secondary amine. Vials of the solutions were placed in a steel reaction vessel and stirred for 3 d under 10 bar of NO gas. The product was precipitated and washed with acetone to recover CD-PA/NO.

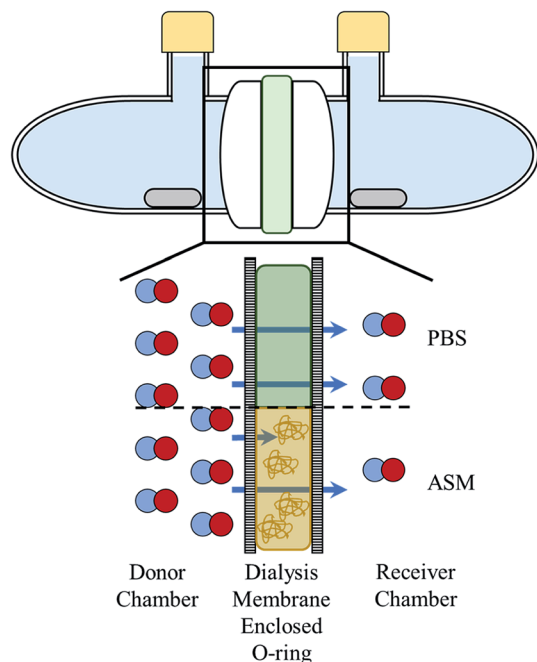
### Diffusion cell

A glass diffusion cell was manufactured by the UNC Chemistry glass shop. Each chamber of the cell had an aperture diameter of 15 mm and could contain up to 11.5 mL of solution. Dialysis membranes (Spectra/Por; 6–8 kDa MWCO) were rehydrated in water for 2 min and positioned on either side of the square O-ring (12 × 12 mm) as depicted in Scheme 1. The O-ring provides a known, reproducible area and volume (1.44 cm<sup>2</sup> and 500 μL, respectively) for the boundary solutions (*i.e.*, PBS and ASM). The O-ring and membranes were sandwiched between the glass diffusion cell chambers and secured with a metal clamp (Scheme 1 and Fig. S1†). Stir bars were added to each chamber, and the ports were sealed with rubber septa and parafilm. Unless mentioned otherwise, the chamber with NO or NO donor at the start of the experiment is referred to as the “donor chamber” with the chamber absent NO (*i.e.*, only PBS) referred to as the “receiver chamber.”

### Nitric oxide diffusion through PBS and ASM

The entire diffusion cell was sparged with argon for 10 min per chamber to displace any air initially present. All solutions were sealed with rubber septa and deoxygenated with argon for 25 min each before addition to the diffusion cell. Donor chamber solutions were prepared by diluting saturated NO solution or by dissolving CD-PA/NO in deoxygenated PBS. Using a syringe, 500 μL of PBS or ASM was injected into the O-ring. The donor and receiver solutions were removed from their sealed containers with a syringe and added to their respective





**Scheme 1** Top: cut-out side view of the side-by-side diffusion cell. Blue: liquid filling the cell chambers; green: square O-ring containing diffusion barrier liquid; grey: stir bars; yellow: rubber septa. Bottom: expanded graphic showing the setup and hypothesized function of the two barrier solutions tested; green is PBS and yellow is ASM.

chambers (11.5 mL). Of note, argon (Ar) gas was used to backfill the containers to prevent oxygen/air from entering the cell. The completed diffusion cell was placed on a multi-position stir plate while stirring each chamber throughout the duration of the experiment.

### Nitrite quantification *via* Griess assay

At each timepoint, 100  $\mu\text{L}$  of solution was removed from the receiver chamber *via* syringe and added to a 96-well plate for Griess assay analysis. Following the completion of the experiment, the solutions sat for 2 h to allow all remaining NO to oxidize to nitrite. Aliquots of the samples (50  $\mu\text{L}$ ) were combined with 50  $\mu\text{L}$  of a 1% w/v sulfanilamide aqueous solution (5% v/v phosphoric acid). The mixture was allowed to react in the dark for 10 min. A 0.1% w/v solution of NED in water (50  $\mu\text{L}$ ) was then added and placed in the dark for 10 min. The ensuing pink azo dye's absorbance was measured at 540 nm. Calibration curves were produced using solutions prepared by serial dilutions of a sodium nitrite standard.

### Calculation of diffusion coefficients

The apparent diffusion coefficient was calculated using the following equation:<sup>28</sup>

$$\ln\left(\frac{C_0}{(C_0 - C)}\right) = \frac{DA}{lV}t \quad (1)$$

where the concentration of NO in the donor chamber and the receiver chamber are denoted as  $C_0$  and  $C$ , respectively

(determined using Griess assay). Area of O-ring opening is  $A$ ;  $l$  is the thickness of the diffusion barrier;  $V$  is the volume of the receiver chamber;  $D$  is the diffusion coefficient;  $t$  is time. A linear relationship between  $\ln(C_0/(C_0 - C))$  and time was exploited to solve for  $D$  (Fig. 1).

### Diffusion of NO through differentiated lung tissue

Differentiated lung tissues (EpiAirway) were purchased from MatTek Corporation (Ashland, MA) and cultured on porous inserts for 14 d prior to delivery. All tissues were grown using the same donor lung tissue and used within 48 h of receipt to limit variation in tissue-to-tissue cell growth and differentiation. Tissue inserts were stored in 1 mL of media (replaced daily) in 6-well plates and incubated (37  $^{\circ}\text{C}$ , 5%  $\text{CO}_2$ ). To prepare the tissues, the apical surface was rinsed twice with 400  $\mu\text{L}$  of sterile PBS to remove any naturally produced mucus. Tissue inserts were placed in 300  $\mu\text{L}$  of TEER buffer (MatTek Corp.) in a 24-well plate, followed by the addition of 100  $\mu\text{L}$  of donor solution (Scheme 2). Samples were taken at select time points by moving the tissues to another well containing a fresh 300  $\mu\text{L}$  of TEER buffer. The used TEER buffer was divided into two aliquots for analysis *via* Griess assay and CD quantification *via* HPLC analysis. Tissues were returned to the incubator between all time points. Application of ASM to the tissue was performed following removal of mucus by pipetting 15  $\mu\text{L}$  of sterile ASM (equivalent to 250  $\mu\text{m}$  thickness) onto the exposed tissue surface prior to the addition of the donor solution.

### Determination of tissue viability *via* colorimetric assay

Immediately following the conclusion of the NO diffusion experiments, the tissues were washed twice with 400  $\mu\text{L}$  of sterile PBS to remove any NO-releasing or control CD-PA. A solution of cell media, MTS, and PMS (105/20/1 v/v/v) was prepared in the absence of light. For each tissue, 300  $\mu\text{L}$  of the MTS solution was added to a 24-well plate, and the tissue insert was placed in the solution. Untreated tissue samples and tissues fixed with 400  $\mu\text{L}$  formaldehyde (10%, v/v) for 6 h were used as the control and blank, respectively. All tissues (samples and controls) were incubated in the dark for 3 h at 37  $^{\circ}\text{C}$ , 5%

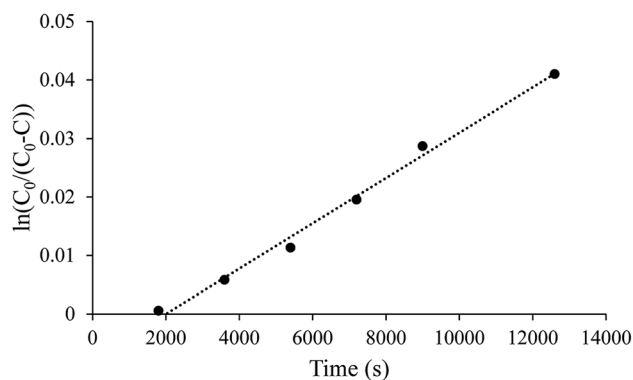
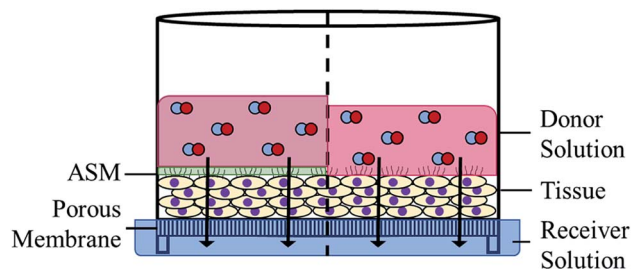


**Fig. 1** Representative linear diffusion trend between the  $\ln(C_0/(C_0 - C))$  and time as expected in eqn (1). All nitrite concentrations were determined using Griess assay.





**Scheme 2** Side view demonstrating the proposed diffusion of NO through human lung tissue. Arrows represent the simplified path of NO released from CD-PA/NO in the donor solution (PBS; pH 7.4) to the receiver solution (TEER buffer) through the tissue mass and porous membrane. Left side shows the addition of 15  $\mu\text{L}$  ASM to the apical side of the tissue prior to the application of the donor solution.

$\text{CO}_2$ . Tissue inserts were removed, and 100  $\mu\text{L}$  aliquots were taken in duplicate for absorbance measurements at 490 nm in a 96-well plate. Tissue viability was calculated as follows:

$$\text{Cell viability (\%)} = \frac{\text{Abs}_{490} - \text{Abs}_{\text{blank}}}{\text{Abs}_{\text{control}} - \text{Abs}_{\text{blank}}} \times 100\% \quad (2)$$

### Quantification of cyclodextrin diffusion via HPLC

Diffusion of CD-PA through the tissue was quantified using high-performance liquid chromatography (HPLC; Agilent Technologies 1260 Infinity II LC System) equipped with a diode array detector (DAD; Agilent Technologies) and an evaporative light scattering detector (ELSD; Agilent Technologies). Aliquots (20  $\mu\text{L}$ ) collected during the tissue diffusion study were injected into the HPLC system for analysis. Ionic buffer components were separated from CD-PA using a C18 column containing 2.7  $\mu\text{m}$  particles (InfinityLab Poroshell 120 EC-C18;  $4.6 \times 100 \text{ mm}$ ). The mobile phase was composed of 100% water for the first 2 min of each analysis to aid in the elution of ionic components. The composition was then adjusted to 50/50 water/acetonitrile over 4 min and held at that ratio for an additional 2 min. The mobile phase was then adjusted back to 100% water in preparation for the next analysis. The mobile phase flow rate was kept constant at  $1.0 \text{ mL min}^{-1}$ . Cyclodextrin elution was monitored via ELSD. Standards were prepared by dissolving CD-PA in buffer ( $0.0125\text{--}0.100 \text{ mg mL}^{-1}$ ) allowing for quantification of CD-PA at concentrations above  $0.0125 \text{ mg mL}^{-1}$ .

### Data analysis

Values for nitrite concentration, CD concentration, diffusion coefficient, and cell viability are represented as the mean  $\pm$  the standard error of the mean. All significance testing was performed via a 2-tailed Student's *t*-test with a minimum of  $p < 0.05$  indicating statistical significance.

## Results and discussion

Diffusion of NO through water, aqueous salt solutions, and polymer blocks has been studied by others using a variety of

methodologies.<sup>26–29</sup> However, the volatility of NO, a diatomic radical, restricts most non-computational diffusion research to simple (*i.e.*, water, saline) solutions or unreactive solids, both of which are not indicative of biological systems. By modifying the conventional side-by-side diffusion cell concept, NO diffusion through proteinaceous solutions (*i.e.*, ASM) was investigated. Dialysis membranes were employed to trap large proteins and molecules (*i.e.*, mucins, DNA, egg yolk emulsion) within the confines of an O-ring, providing a known, reproducible volume for the biological fluid (*i.e.*, ASM) without overly complex designs (Scheme 1).

### NO diffusion coefficients through PBS and ASM

Initial testing using this diffusion methodology required confirmation that the observed diffusion coefficients in saline (*i.e.*, PBS) were consistent with previous literature. As discussed in previous studies, significant care was taken to purge the system of oxygen to prevent the spontaneous oxidation of NO, which would skew the diffusion coefficient.<sup>28,42</sup> All solutions and the assembled diffusion cell were sparged with Ar to displace residual air. Donor solutions were prepared by diluting PBS saturated with NO into deoxygenated PBS. Over 6 h, NO diffused across the PBS diffusion barrier encompassed by the dialysis membrane to the receiver chamber. The relationship between  $\ln(C_0/(C_0 - C))$  and time was linear as predicted by the equation derived from Fick's first law (Fig. 1 and eqn (1)). The delay prior to the first detectable point in Fig. 1 is attributed to the thick, diffusion barrier, which necessitated a significant amount of time ( $\sim 1800 \text{ s}$ ) to enable quantifiable levels of NO to reach to the receiver chamber. The calculated apparent diffusion coefficient of  $(1.15 \pm 0.25) \times 10^{-5} \text{ cm}^2 \text{ s}^{-1}$  corresponds to the general range of accepted literature values (Table 1).<sup>26,27,29</sup> As such, the diffusion cell and methodology were determined to accurately measure the diffusion of NO. Of note, the methodology used to study diffusion can influence the calculated coefficient, resulting in a large range of literature values.<sup>30,31,43,44</sup>

As previously stated, simple saline solutions are not indicative of a biological environment. Artificial sputum medium, a common CF mucus analog, was thus used to replace saline. By introducing ASM as the barrier solution, changes in the

**Table 1** Diffusion coefficients of NO through various aqueous media determined with different measurement techniques from this work and comparable literature

Diffusion medium	Diffusion coefficient ( $\times 10^{-5} \text{ cm}^2 \text{ s}^{-1}$ )	Reference
Water	$2.21 \pm 0.02$	27 <sup>b</sup>
	2.07	26 <sup>d</sup>
Phosphate buffer <sup>a</sup>	3.5	29 <sup>c</sup>
PBS	$2.21 \pm 0.04$	27 <sup>b</sup>
	$1.15 \pm 0.25$	This work <sup>e</sup>
ASM	$0.92 \pm 0.05$	This work <sup>e</sup>

<sup>a</sup> 0.1 N. <sup>b</sup> Diffusion across liquid contained in silastic membrane. <sup>c</sup> Determined via chronoamperometric measurements. <sup>d</sup> Collapse of NO bubbles in water. <sup>e</sup>  $N = 7$ .





measured diffusion characteristics would highlight the interactions of NO with the added biological components. As shown in Table 1, the calculated apparent diffusion coefficient through ASM exhibited a statistically significant decrease to  $(9.25 \pm 0.51) \times 10^{-6} \text{ cm}^2 \text{ s}^{-1}$ , slightly greater than reported values through other biological systems (*e.g.*, diffusion across aortic wall).<sup>45</sup> The slower diffusion was attributed to two primary factors: physical obstruction and protein scavenging. Mucin proteins, the primary solid component of ASM, are exceedingly large molecules (10–40 MDa) that can readily obstruct the diffusion pathway of NO through the formation of a mucin mesh (20–200 nm pores).<sup>46</sup> Additionally, NO is known to react with multiple biologically-relevant components, including thiols on cysteine and glutathione and heme centers.<sup>21,22</sup> The collision of free NO with a disulfide bond, a functional group in high concentration throughout the mucin backbone, may reduce the bond to form a nitrosothiol.<sup>32</sup> While this route is a useful characteristic of NO regarding its potential as a mucolytic agent, it is important to note that the initial flux of NO will be stunted by active consumption prior to reaching such target. Furthermore, the hindered diffusion through ASM will only be exacerbated with the concentration of the CF mucus with disease progression, due to the increasing percentage of mucins and DNA. Significant decreases in diffusion coefficients through ASM suggest that modified dosages will be necessary to compensate for *in vivo* mucus conditions and disease state.

### Diffusion from an extended-release macromolecular NO donor

Although it was shown that ASM impedes the diffusion of NO, the NO source evaluated was NO-saturated PBS, which is not therapeutically relevant. Therefore, we sought to further investigate NO diffusion originating from an extended-release system with antibacterial activity. Our lab has previously developed a number of biopolymer scaffolds capable of storing and releasing NO over extended periods to provide targeted therapeutic doses.<sup>8,37,38,47</sup> For example, NO donor-modified  $\beta$ -cyclodextrin exhibited the ability to eradicate bacteria while eliciting minimal cytotoxicity towards mammalian cells,<sup>38</sup> making it an appealing method for therapeutic NO delivery. In this work, the NO-releasing propylamine-modified variant (CD-PA/NO) was selected due to its ability to deliver high NO payloads ( $0.61 \pm 0.05 \mu\text{mol mg}^{-1}$ ) with a moderate half-life ( $1.73 \pm 0.24 \text{ h}$ ).<sup>38</sup>

Donor chamber solutions were prepared using 4.6 mg of CD-PA/NO in 12 mL of deoxygenated PBS ( $\sim 0.38 \text{ mg mL}^{-1}$ ), a concentration well below any cytotoxic level.<sup>38</sup> In contrast to the immediate presence of the NO in the NO-saturated PBS tests, NO was released from CD-PA/NO throughout the entirety of the experiment due to its prolonged release profile. As a result, the apparent diffusion coefficient was not determined because the NO concentration in the donor chamber changed constantly. Rather, NO diffusion was observed as a general rate (*i.e.*, increasing concentration over time) and compared between the two boundary solutions (Fig. 2). In accordance with the diffusion coefficients determined using NO-saturated PBS, NO released from CD-PA/NO accumulated in the receiver

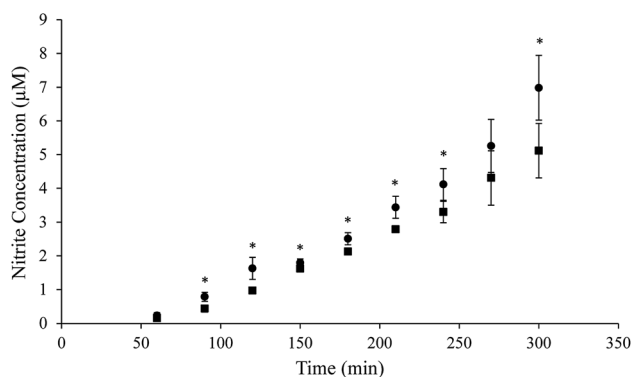


Fig. 2 Diffusion of NO, released over time from CD-PA/NO, through a barrier of PBS (circles) or ASM (squares). Nitrite concentrations, analogous for the presence of NO, were quantified via Griess assay. \* $p < 0.05$ .

chamber at a significantly faster rate at most time points when diffusing through PBS as compared to ASM. Of note, the initial (60 min) timepoint was too early to be significant using the Griess assay as the detection method due to an inadequate limit of detection.<sup>21,48,49</sup> In addition, high error at 270 min, resulting from the random nature of diffusion, was attributed to its lack of significance.<sup>50</sup> Overall, NO released from the donor molecule aptly followed the diffusion characteristics seen using a bulk NO source (*i.e.*, NO-saturated PBS). Regardless of whether large quantities of NO are present initially or released over time, the diffusion in ASM proved to be impeded compared to PBS.

### Diffusion through differentiated lung tissue

While ASM was chosen to represent the initial diffusion barrier in the lungs (*i.e.*, mucus), some NO may proceed to interact with underlying lung tissue. The exterior layer of lung tissue is composed of ciliated epithelial cells and mucin-secreting goblet cells.<sup>3</sup> Understanding diffusion through these increasingly complex environments is crucial to parsing out NO's true therapeutic potential and cytocompatibility. The diffusion of NO released from CD-PA/NO was monitored over a 6 h exposure to the apical (*i.e.*, tissue–air interface) side of the tissue utilizing a commercially available differentiated lung tissue 3-D model. Simultaneously, the concentrations of NO, measured as nitrite *via* Griess assay, and the CD-PA scaffold, quantified using HPLC, were monitored at 2 h intervals (Table 2). Measurable nitrite concentrations were observed at all timepoints when  $2.0 \text{ mg mL}^{-1}$  CD-PA/NO, a bactericidal concentration, was present in the donor solution. The diffusion of NO was relatively consistent over the first 4 h, with approximately  $28 \mu\text{M}$  increases at the 2 and 4 h timepoints followed by a  $\sim 40 \mu\text{M}$  increase at 6 h. This boost in nitrite was attributed to the prolonged release of NO from the CD-PA/NO throughout the entire 6 h exposure, leading to a buildup of NO in the donor solution at the later timepoints. Additionally, biomolecules scavenging with NO would be diminished from NO's prolonged presence (*e.g.*, thiols previously converted to *S*-nitrosothiols). As expected, when NO was absent (*i.e.*,  $2.0 \text{ mg mL}^{-1}$  CD-PA), negligible quantities of



**Table 2** Concentrations of nitrite and cyclodextrin diffused across differentiated lung tissue at various timepoints and the percent tissue viability following a 6 h exposure to CD-PA/NO and CD-PA/NO<sup>a</sup>

Donor solution <sup>b</sup>	Timepoint range (h)	[Nitrite] (μM)	[Nitrite] <sup>c</sup> (%)	[CD] (mg mL <sup>-1</sup> )	[CD] <sup>c</sup> (%)	Tissue viability <sup>d</sup> (%)
2.0 mg mL <sup>-1</sup> CD-PA/NO	0–2	27.5 ± 1.3	4.7 ± 0.2	N. D. <sup>e</sup>	<0.65 <sup>e</sup>	113.1 ± 9.0
	2–4	56.8 ± 1.3	7.3 ± 0.2	N. D.	<0.65	
	4–6	95.8 ± 2.2	10.6 ± 0.2	0.026 ± 0.002* <sup>†</sup>	1.3 ± 0.1* <sup>†</sup>	
2.0 mg mL <sup>-1</sup> CD-PA	0–2	#	#	N. D.	<0.65	107.0 ± 8.9
	2–4	#	#	N. D.	<0.65	
	4–6	0.2 ± 0.2	0.0 ± 0.0	0.071 ± 0.014 <sup>†</sup>	3.5 ± 0.7 <sup>†</sup>	
2.0 mg mL <sup>-1</sup> CD-PA/NO + 15 μL ASM	0–2	28.1 ± 1.3	4.8 ± 0.2	N. D.	<0.65	101.3 ± 5.3
	2–4	59.1 ± 1.7	7.6 ± 0.2	N. D.	<0.65	
	4–6	98.6 ± 1.3	10.9 ± 0.1	0.020 ± 0.002*	1.0 ± 0.1*	

<sup>a</sup> *N* = 3 for all reported values. <sup>b</sup> All donor solutions were made in PBS (pH 7.4) and 100 μL of the solutions were added to the apical side of the tissue. <sup>c</sup> Percentage of the nitrite or CD that diffused compared to the total NO released up to that time or initial concentration of CD in donor solution. <sup>d</sup> Viability only measured following entire 6 h exposure. <sup>e</sup> Values were below the detection limit of our HPLC method which was <0.013 mg mL<sup>-1</sup> CD (or 0.65%). <sup>†</sup> Griess assay was not performed at these timepoints. \**p* < 0.01 compared to CD-PA. <sup>†</sup> *p* < 0.05 compared to CD-PA/NO + ASM.

nitrite were detected in the receiver solutions following exposure (Table 2). Conversely, the amount of CD-PA detected in the receiver solution was only detectable at the 6 h timepoint for both exposures and was found at greater concentrations following treatment with control (non-NO-releasing) CD-PA tests as compared to CD-PA/NO. In contrast with NO, CD-PA's larger size and significantly lower diffusion coefficient ( $\sim 0.3 \times 10^{-5} \text{ cm}^2 \text{ s}^{-1}$ ) resulted in the noticeable lag across the tissue.<sup>51–53</sup> The discrepancy between concentrations following exposure to CD-PA and CD-PA/NO were likely a result of the charge disparity. The zwitterionic *N*-diazeniumdiolate moiety appended to the secondary amine facilitating the storage of NO on the CD backbone induces a net negative charge that likely slows the molecules' diffusion through the tissue layer. Once the NO is expended, the CD-PA has no net charge and diffuses more easily. Furthermore, enzymes with the capability to degrade polysaccharides (*e.g.*,  $\alpha$ -amylase<sup>54</sup>) may have assisted in slowing CD-PA's diffusion through the tissue.

Not to be overlooked, *in vivo* lung tissue is coated with a layer of mucus. In order to simulate the mucus lining structure, a layer of ASM was pipetted onto the tissue prior to dosing with CD-PA/NO. A volume equivalent to 250 μm thick mucus (15 μL of ASM) was selected as such thickness is representative of a naturally produced mucus layer.<sup>55</sup> Contrary to the isolated diffusion experiments using the diffusion cell, nitrite concentrations at each timepoint were found to not be statistically different from the tissues without ASM (Table 2). This lack of variation was attributed to the volume of donor solution added (100 μL). As a result, the water-soluble ASM components were dispersed throughout the PBS rather than localizing at the tissue surface, decreasing their influence on NO diffusion.<sup>56</sup> A significant reduction in CD-PA diffusion in the presence of the ASM layer was observed compared to tissue without the ASM layer. The inherent slower diffusion, larger size, and net charge of the CD-PA/NO may have facilitated more interaction with the dispersed mucin mesh, while the changes in NO diffusion are undetectable with this detection methodology. Of note, no

cytotoxicity was observed for any tissues exposed to these antibacterial concentrations of CD-PA/NO (Table 2).

In order to compare the impact of PBS, ASM, and tissue barriers on NO diffusion, the concentration of nitrite at the 6 h timepoint was normalized to the total volume of the diffusion barrier. Under the controlled diffusion cell system, the normalized concentration of NO released from CD-PA/NO that accumulated across the barrier layer over 6 h was  $3.62 \pm 0.50$  and  $2.65 \pm 0.42 \text{ μM}$  for PBS and ASM, respectively. Across the more dense tissue model, the normalized concentration was significantly reduced to  $0.48 \pm 0.01 \text{ μM}$  after 6 h. As expected, the tissue resulted in a substantial barrier to NO diffusion compared to the aqueous solutions, although the high lipophilicity of NO still allowed for measurable quantities to diffuse through the thin ( $\sim 4$  cells thick) tissue layer.<sup>57</sup>

## Conclusions

Utilizing a modified side-by-side diffusion cell, the diffusion coefficient for NO through ASM was found to be significantly lower than through PBS due to obstruction from the mucin mesh and reactive nature of NO radicals in biological solutions. Differences in diffusion characteristics were further confirmed by observing the rate of NO diffusion following its active release from a macromolecular NO donor molecule, CD-PA/NO. A significantly reduced rate in NO accumulation relative to both PBS and ASM was observed through *in vitro* lung tissue. While NO is a promising antibacterial agent, these data demonstrate how increasing biological complexity impacts NO diffusion and thus its potential for antibacterial action. Work exploring potential therapeutic roles of NO must carefully consider the relevant physiological environment. While the diffusion cell methodology employed herein elucidated the impact of mucus on the diffusion of NO, it can easily be applied to other biological solutions containing large proteins or biomolecules (*e.g.*, from simulated wound fluid or blood) to better understand the effect of those environments on NO diffusion and activity. Moreover, this methodology provides



a simple way to measure the diffusion coefficient of volatile, dissolved gases (e.g., hydrogen sulfide, carbon monoxide).

## Conflicts of interest

The corresponding author declares competing financial interest. Mark Schoenfisch is a co-founder, member of the board of directors, and maintains a financial interest in KnowBIO, LLC and Vast Therapeutics, Inc. Vast Therapeutics is commercializing macromolecular nitric oxide storage and release scaffolds for the treatment of cystic fibrosis.

## Acknowledgements

Funding for this research was provided by the National Institutes of Health (DE025207), Cystic Fibrosis Foundation (Schoen18G0), and KnowBIO, LLC.

## References

- 1 D. J. Hassett, J. Cuppoletti, B. Trapnell, S. V. Lymar, J. J. Rowe, S. Yoon, G. M. Hilliard, K. Parvatiyar, M. C. Kamani, D. J. Wozniak, S. H. Hwang, T. R. McDermott and U. A. Ochsner, Anaerobic metabolism and quorum sensing by *Pseudomonas aeruginosa* biofilms in chronically infected cystic fibrosis airways: rethinking antibiotic treatment strategies and drug targets, *Adv. Drug Delivery Rev.*, 2002, **54**, 1425–1443.
- 2 G. R. Cutting, Cystic fibrosis genetics: from molecular understanding to clinical application, *Nat. Rev. Genet.*, 2015, **16**, 45–56.
- 3 F. Ratjen, S. C. Bell, S. M. Rowe, C. H. Goss, A. L. Quittner and A. Bush, Cystic Fibrosis, *Nat. Rev. Dis. Primers*, 2015, **1**, 1–19.
- 4 B. K. Rubin, Cystic Fibrosis 2017—The Year in Review, *Respir. Care*, 2018, **63**, 238–241.
- 5 B. K. Rubin, Mucus structure and properties in cystic fibrosis, *Paediatr. Respir. Rev.*, 2007, **8**, 4–7.
- 6 J. A. Voynow and B. K. Rubin, Mucins, mucus, and sputum, *Chest*, 2009, **135**, 505–512.
- 7 D. B. Hill, R. F. Long, W. J. Kissner, E. Atieh, I. C. Garbarine, M. R. Markovetz, N. C. Fontana, M. Christy, M. Habibpour, R. Tarran, M. G. Forest, R. C. Boucher and B. Button, Pathological mucus and impaired mucus clearance in cystic fibrosis patients result from increased concentration, not altered pH, *Eur. Respir. J.*, 2018, **52**, 1801297.
- 8 K. P. Reighard and M. H. Schoenfisch, Antibacterial action of nitric oxide-releasing chitosan oligosaccharides against *Pseudomonas aeruginosa* under aerobic and anaerobic conditions, *Antimicrob. Agents Chemother.*, 2015, **59**, 6506–6513.
- 9 P. S. Stewart and J. W. Costerton, Antibiotic resistance of bacteria in biofilms, *Lancet*, 2001, **358**, 135–138.
- 10 S. Kirkby, K. Novak and K. McCoy, Aztreonam (for inhalation solution) for the treatment of chronic lung infections in patients with cystic fibrosis: an evidence-based review, *Core Evidence*, 2011, **6**, 59–66.
- 11 C. Koerner-Rettberg and M. Ballmann, Colistimethate sodium for the treatment of chronic pulmonary infection in cystic fibrosis: an evidence-based review of its place in therapy, *Core Evidence*, 2014, **9**, 99–112.
- 12 V. Waters and F. Ratjen, Multidrug-resistant organisms in cystic fibrosis: management and infection-control issues, *Expert Rev. Anti-Infect. Ther.*, 2006, **4**, 807–819.
- 13 K. Poole, Aminoglycoside resistance in *Pseudomonas aeruginosa*, *Antimicrob. Agents Chemother.*, 2005, **49**, 479–487.
- 14 A. W. Carpenter and M. H. Schoenfisch, Nitric oxide release: part II. Therapeutic applications, *Chem. Soc. Rev.*, 2012, **41**, 3742–3752.
- 15 F. C. Fang, Mechanisms of nitric oxide-related antimicrobial activity, *J. Clin. Invest.*, 1997, **99**, 2818–2825.
- 16 F. C. Fang, Antimicrobial reactive oxygen and nitrogen species: concepts and controversies, *Nat. Rev. Microbiol.*, 2004, **2**, 820–832.
- 17 B. J. Privett, A. D. Broadnax, S. J. Bauman, D. A. Riccio and M. H. Schoenfisch, Examination of bacterial resistance to exogenous nitric oxide, *Nitric Oxide*, 2012, **26**, 169–173.
- 18 K. P. Reighard, C. Ehre, Z. L. Rushton, M. J. R. Ahonen, D. B. Hill and M. H. Schoenfisch, Role of Nitric Oxide-Releasing Chitosan Oligosaccharides on Mucus Viscoelasticity, *ACS Biomater. Sci. Eng.*, 2017, **3**, 1017–1026.
- 19 M. J. R. Ahonen, D. B. Hill and M. H. Schoenfisch, Nitric Oxide-Releasing Alginates as Mucolytic Agents, *ACS Biomater. Sci. Eng.*, 2019, **5**, 3409–3418.
- 20 S. Archer, Measurement of nitric oxide in biological models, *FASEB J.*, 1993, **7**, 349–360.
- 21 R. A. Hunter, W. L. Storm, P. N. Coneski and M. H. Schoenfisch, Inaccuracies of nitric oxide measurement methods in biological media, *Anal. Chem.*, 2013, **85**, 1957–1963.
- 22 A. J. Gow and J. S. Stamler, Reactions between nitric oxide and haemoglobin under physiological conditions, *Nature*, 1998, **391**, 169–173.
- 23 C. E. Cooper, Nitric oxide and iron proteins, *Biochim. Biophys. Acta, Bioenerg.*, 1999, **1411**, 290–309.
- 24 N. Schweighofer and G. Ferriol, Diffusion of nitric oxide can facilitate cerebellar learning: a simulation study, *Proc. Natl. Acad. Sci. U. S. A.*, 2000, **97**, 10661–10665.
- 25 J. R. Lancaster Jr, A tutorial on the diffusibility and reactivity of free nitric oxide, *Nitric Oxide*, 1997, **1**, 18–30.
- 26 D. L. Wise and G. Houghton, Diffusion coefficients of neon, krypton, xenon, carbon monoxide and nitric oxide in water at 10–60 °C, *Chem. Eng. Sci.*, 1968, **23**, 1211–1216.
- 27 I. G. Zacharia and W. M. Deen, Diffusivity and Solubility of Nitric Oxide in Water and Saline, *Ann. Biomed. Eng.*, 2005, **33**, 214–222.
- 28 K. A. Mowery and M. E. Meyerhoff, The transport of nitric oxide through various polymeric matrices, *Polymer*, 1999, **40**, 6203–6207.
- 29 S. A. Bhat, S. A. Pandit, M. A. Rather, G. M. Rather, N. Rashid, P. P. Ingole and M. A. Bhat, Self-assembled AuNPs on sulphur-doped graphene: a dual and highly efficient



- electrochemical sensor for nitrite ( $\text{NO}_2^-$ ) and nitric oxide (NO), *New J. Chem.*, 2017, **41**, 8347–8358.
- 30 A. Denicola, J. M. Souza, R. Radi and E. Lissi, Nitric oxide diffusion in membranes determined by fluorescence quenching, *Arch. Biochem. Biophys.*, 1996, **328**, 208–212.
  - 31 N. I. Ikhsan, P. Rameshkumar and N. M. Huang, Electrochemical properties of silver nanoparticle-supported reduced graphene oxide in nitric oxide oxidation and detection, *RSC Adv.*, 2016, **6**, 107141–107150.
  - 32 M. Boegh and H. M. Nielsen, Mucus as a Barrier to Drug Delivery – Understanding and Mimicking the Barrier Properties, *Basic Clin. Pharmacol. Toxicol.*, 2015, **116**, 179–186.
  - 33 T. Samad, J. Y. Co, J. Witten and K. Ribbeck, Mucus and Mucin Environments Reduce the Efficacy of Polymyxin and Fluoroquinolone Antibiotics against *Pseudomonas aeruginosa*, *ACS Biomater. Sci. Eng.*, 2019, **5**, 1189–1194.
  - 34 B. V. Worley, K. M. Schilly and M. H. Schoenfisch, Antibiofilm efficacy of dual-action nitric oxide-releasing alkyl chain modified poly(amidoamine) dendrimers, *Mol. Pharm.*, 2015, **12**, 1573–1583.
  - 35 D. A. Riccio and M. H. Schoenfisch, Nitric oxide release: part I. Macromolecular scaffolds, *Chem. Soc. Rev.*, 2012, **41**, 3731–3741.
  - 36 D. J. Suchyta and M. H. Schoenfisch, Encapsulation of N-diazoniumdiolates within liposomes for enhanced nitric oxide donor stability and delivery, *Mol. Pharm.*, 2015, **12**, 3569–3574.
  - 37 M. J. R. Ahonen, D. J. Suchyta, H. Zhu and M. H. Schoenfisch, Nitric Oxide-Releasing Alginates, *Biomacromolecules*, 2018, **19**, 1189–1197.
  - 38 H. Jin, L. Yang, M. J. R. Ahonen and M. H. Schoenfisch, Nitric Oxide-Releasing Cyclodextrins, *J. Am. Chem. Soc.*, 2018, **140**, 14178–14184.
  - 39 Y. Lu, A. Shah, R. A. Hunter, R. J. Soto and M. H. Schoenfisch, S-Nitrosothiol-modified nitric oxide-releasing chitosan oligosaccharides as antibacterial agents, *Acta Biomater.*, 2015, **12**, 62–69.
  - 40 D. D. Sriramulu, H. Lünsdorf, J. S. Lam and U. Römling, Microcolony formation: a novel biofilm model of *Pseudomonas aeruginosa* for the cystic fibrosis lung, *J. Med. Microbiol.*, 2005, **54**, 667–676.
  - 41 S. Kirchner, J. L. Fothergill, E. A. Wright, C. E. James, E. Mowat and C. Winstanley, Use of artificial sputum medium to test antibiotic efficacy against *Pseudomonas aeruginosa* in conditions more relevant to the cystic fibrosis lung, *J. Visualized Exp.*, 2012, **64**, e3857.
  - 42 H. Ren, J. L. Bull and M. E. Meyerhoff, Transport of Nitric Oxide (NO) in Various Biomedical grade Polyurethanes: Measurements and Modeling Impact on NO Release Properties of Medical Devices, *ACS Biomater. Sci. Eng.*, 2016, **2**, 1483–1492.
  - 43 J. M. Vanderkooi, W. W. Wright and M. Erecinska, Nitric oxide diffusion coefficients in solutions, proteins and membranes determined by phosphorescence, *Biochim. Biophys. Acta, Bioenerg.*, 1994, **1207**, 249–254.
  - 44 S. Pokharel, N. Pantha and N. P. Adhikari, Diffusion coefficients of nitric oxide in water: a molecular dynamics study, *Int. J. Mod. Phys. B*, 2016, **30**, 1650205.
  - 45 X. Liu, P. Srinivasan, E. Collard, P. Grajdeanu, J. L. Zweier and A. Friedman, Nitric oxide diffusion rate is reduced in the aortic wall, *Biophys. J.*, 2008, **94**, 1880–1889.
  - 46 S. S. Olmsted, J. L. Padgett, A. I. Yudin, K. J. Whaley, T. R. Moench and R. A. Cone, Diffusion of Macromolecules and Virus-Like Particles in Human Cervical Mucus, *Biophys. J.*, 2001, **81**, 1930–1937.
  - 47 Y. Lu, D. L. Slomberg and M. H. Schoenfisch, Nitric oxide-releasing chitosan oligosaccharides as antibacterial agents, *Biomaterials*, 2014, **35**, 1716–1724.
  - 48 P. N. Coneski and M. H. Schoenfisch, Nitric oxide release: part III. Measurement and reporting, *Chem. Soc. Rev.*, 2012, **41**, 3753–3758.
  - 49 E. M. Hetrick and M. H. Schoenfisch, Analytical Chemistry of Nitric Oxide, *Annu. Rev. Anal. Chem.*, 2009, **2**, 409–433.
  - 50 D. M. Himmelblau, Diffusion of Dissolved Gases in Liquids, *Chem. Rev.*, 1964, **64**, 527–550.
  - 51 G. M. Pavlov, E. V. Korneeva, N. A. Smolina and U. S. Schubert, Hydrodynamic properties of cyclodextrin molecules in dilute solutions, *Eur. Biophys. J.*, 2010, **39**, 371–379.
  - 52 K. S. Cameron and L. Fielding, NMR diffusion coefficient study of steroid-cyclodextrin inclusion complexes, *Magn. Reson. Chem.*, 2002, **40**, 106–109.
  - 53 L. Paduano, R. Sartorio, V. Vitagliano and L. Costantino, Diffusion properties of cyclodextrins in aqueous solution at 25 °C, *J. Solution Chem.*, 1990, **19**, 31–39.
  - 54 A. Fetzner, S. Böhm, S. Schreder and R. Schubert, Degradation of raw or film-incorporated  $\beta$ -cyclodextrin by enzymes and colonic bacteria, *Eur. J. Pharm. Biopharm.*, 2004, **58**, 91–97.
  - 55 A. L. Oldenburg, R. K. Chhetri, D. B. Hill and B. Button, Monitoring airway mucus flow and ciliary activity with optical coherence tomography, *Biomed. Opt. Express*, 2012, **3**, 1978–1992.
  - 56 H. Matsui, V. E. Wagner, D. B. Hill, U. E. Schwab, T. D. Rogers, B. Button, R. M. Taylor, R. Superfine, M. Rubinstein, B. H. Iglewski and R. C. Boucher, A physical linkage between cystic fibrosis airway surface dehydration and *Pseudomonas aeruginosa* biofilms, *Proc. Natl. Acad. Sci. U. S. A.*, 2006, **103**, 18131–18136.
  - 57 J. L. Wallace and M. J. S. Miller, Nitric oxide in mucosal defense: a little goes a long way, *Gastroenterology*, 2000, **119**, 512–520.

